Heliyon 11 (2025) e42577

Contents lists available at ScienceDirect

Heliyon

journal homepage: www.cell.com/heliyon

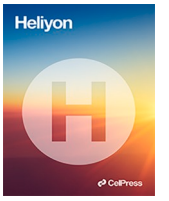

Research article

Exploring the therapeutic potential of Danggui Shaoyao San in nephrotic syndrome: Impact on skin sodium content and renal function

Qingzhen Xiang [a], Lianghou Ni [a], Zaiping Xu [a], Xiaowen Ma [a], Yunlai Wang [a,b,c], Zihua Xuan [a,b], Fan Xu [a,b,c,*]

[a] School of Pharmacy, Anhui University of Chinese Medicine, Hefei, China
[b] Anhui Province Key Laboratory of Chinese Medicinal Formula, Hefei, China
[c] Institute for Pharmacodynamics and Safety Evaluation of Chinese Medicine, Anhui Academy of Chinese Medicine, Hefei, China

A B S T R A C T

The purpose of this study was to explore the mechanism of sodium transport in the skin of rats with nephrotic syndrome (NS) and the intervention effect of Danggui Shaoyao San (DSS). NS model was established by tail vein injection of adriamycin (ADR), and different doses of DSS, vascular endothelial growth factor receptor-3 (VEGFR-3) inhibitor Levatinib and diuretic amiloride were given for intervention. We analysed serum biochemical parameters, urine sodium, skin sodium and glycosaminoglycan (GAG), lymphatic vessel density, and the expression and mRNA levels of key proteins involved in lymphangiogenesis. The results showed that DSS treatment not only significantly reduced the content of sodium ions in the skin of NS rats, but also effectively alleviated the pathological damage of the kidney, improved proteinuria and promoted the excretion of sodium in urine. At the same time, Levatinib can reduce the content of sodium ions in the skin of NS rats by inhibiting lymphangiogenesis, while amiloride can improve the state of sodium retention in the body and reduce the level of sodium ions in the skin by promoting the excretion of sodium ions in the urine of NS rats. Especially important, DSS can effectively inhibit the proliferation of renal cortical lymphatic vessels, down-regulate the expression of lymphangiogenesis related proteins and mRNA, promote urinary sodium excretion, and inhibit the transport of sodium ions from kidney to skin.

In summary, this study reveals that during sodium retention in NS rats, sodium ions can be further transported to the skin for storage through increased lymph in the kidney, and DSS can inhibit renal lymphangiogenesis, promote urinary sodium excretion, and reduce the content of sodium ions in the skin, which provides a novel and potential strategy for the treatment of NS edema.

1. Introduction

The main clinical manifestations of nephrotic syndrome (NS) include edema, proteinuria, hypoproteinaemia, and hyperlipidaemia [1,2]. To date, the pathogenesis of NS is not well understood and is considered complex. Current treatment options for NS mainly include glucocorticoids, cytotoxic medications, and immunosuppressive medications, which can cause serious side effects such as fungal infection and organ toxicity [3,4]. Thus, it is critical to find novel and effective treatments for NS to prevent or delay it.

Sodium plays a crucial role in maintaining the body's internal environment and regulating blood pressure. The kidneys are responsible for maintaining the stability of blood volume and blood pressure by absorbing and excreting sodium and water [5–10]. Recent studies have revealed that NS animals exhibit a substantial reduction in urinary sodium excretion while simultaneously maintaining a stable blood sodium concentration, indicating the accumulation of sodium within the body [11,12]. Studies have shown that sodium levels are significantly increased in the skin and muscle tissue of experimental animals fed a high-salt diet [13]. This

* Corresponding author. School of Pharmacy, Anhui University of Chinese Medicine, Longzihu Road 350, Hefei, Anhui, 230012, China. xufanahcm@qq.com

https://doi.org/10.1016/j.heliyon.2025.e42577
Received 13 August 2023; Received in revised form 7 February 2025; Accepted 7 February 2025
Available online 10 February 2025

sodium binds to GAG in the skin, leading to their storage in the skin. When the skin is exposed to a hypertonic environment caused by factors such as a high salt diet or high sugar intake, macrophage aggregation and the secretion of tonicity-responsive binding-protein (TonEBP) are triggered. This, in turn, leads to the secretion of vascular endothelial growth factor-C (VEGF-C) by macrophages [14]. VEGF-C can bind to VEGFR-3, promoting lymphatic vessel growth and function, lymphatic vessel endothelial hyaluronan receptor-1 (LYVE-1) is the main marker of lymphatic vessels. The lymphatic system plays an essential role in tissue fluid homeostasis, immunosurveillance, lipid metabolism, and inflammation [15]. Moreover, the kidneys can also undergo similar reactions in a hypertonic environment. Therefore, whether there is also an increase in sodium ions in the skin of rats with NS is unclear, and further investigations of the underlying mechanism are needed.

Danggui Shaoyao San (DSS) is a well-known Chinese herbal medicine documented in the Synopsis of the Golden Chamber. DSS consists of 6 herbs, Danggui (*Angelica sinensis* [Oliv.] *Diels*), Baishao (*Paeonia lactiflora* Pall.), Chuanxiong (*Ligusticum chuanxiong* Hort), Baizhu (*Atractylodes macrocephala* Koidz.), Fuling (*Poria cocos* [Schw.] Wolf), and Zexie (*Alisma orientale* [Sam.] Juzep.) at a ratio of 3:16:8:4:4:8. In China, DSS is commonly used to treat dysmenorrhea, and several previous studies have demonstrated its potential for improving Alzheimer's disease [16,17]. Additionally, DSS is also employed in the treatment of NS [18]. We aimed to examine the effects of DSS on NS and explore the possible molecular mechanism by which DSS affects the sodium content in the skin.

2. Materials and methods

2.1. Materials

The 6 raw herbs of DSS were obtained from Guanghe Pharmaceutical Co., Ltd (Anhui, China). ADR was purchased from Hanhui Pharmaceutical Co., Ltd (Zhejiang, China). Amiloride and lenvatinib were obtained from McLean Biochemical Technology Co., Ltd (Shanghai, China). Caesium chloride and nitric acid were obtained from Sigma-Aldrich (St. Louis, MO, USA). BCA protein quantification kits were purchased from Leigen Biotechnology Co., Ltd. (Beijing, China). Antibodies against TonEBP, LYVE-1, VEGF-C, and VEGFR-3 were purchased from Novus Biotechnology Co., Ltd (Colorado, USA).

2.2. Preparation of DSS

These herbs were mixed at a ratio of 3:16:8:4:4:8 for extract preparation. The DSS was soaked in 10 vol of 75 % ethanol for 2 h followed by decocting for 1.5 h. Afterwards, the filtrate was collected, and the filter residue was decocted with 8 vol of 75 % ethanol for another 1.5 h. The extracted solutions were evaporated under vacuum (45 °C) to remove ethanol, and the remaining aqueous solution was concentrated to obtain DSS extract solutions (1.72 g/mL, 0.86 g/mL, and 0.43 g/mL).

2.3. Animals and sample collection

Male Sprague–Dawley rats (300–320 g) were acquired from Pizhou Dongfang Breeding Company. The experimental animals were housed at a temperature of 23 ± 1 °C with a relative humidity of 50%–60 %. The animal research conducted in this study was approved by the Animal Ethics Committee of the Anhui University of Chinese Medicine (licence number: AHUCM-rats-2021068).

After 1 week of acclimatization, the rats were injected with ADR (6 mg/kg) to establish an NS model. Six rats were assigned to the normal group, while the remaining rats were divided into six groups: the model group, levatinib group (50 mg/kg/d), amiloride group (4 mg/kg/d), low dose of DSS (DSS-L) group (4.3 g/kg/d), medium dose of DSS (DSS-M) group (8.6 g/kg/d), and high dose of DSS (DSS-H) group (17.2 g/kg/d). All groups received oral administration via gavage for 4 weeks. During the 4 weeks, the normal group and model group were given equal amounts of purified water (10 mL/kg/d).

At the end of treatment, the animals were kept in an empty cage without bedding to collect fresh stool samples in tubes. The rats were subjected to 12 h of fasting before they were sacrificed. Anaesthesia with 2 % pentobarbital sodium was administered, and blood was collected from the abdominal aorta and centrifuged to yield serum samples. The kindey and skin were precisely dissected. All the samples were immersed immediately in liquid nitrogen and stored at −80 °C for further analysis.

2.4. Analysis of biochemical parameters

The total protein (TP), albumin (ALB), total cholesterol (TC), triglyceride (TG), urea nitrogen (BUN), and creatinine (CR) levels were determined with commercial kits on a biochemical automatic analyser. The levels urinary sodium and urinary protein were quantified using assay kits following the manufacturer's instructions.

2.5. Histological analysis

Kidney samples were fixed in 4 % paraformaldehyde and then embedded in paraffin. Sections of 3 μm thickness were cut from the paraffin-embedded samples. The sections were subsequently stained with haematoxylin/eosin (H&E) and finally, analysed by a microscope (Nikon, Japan).

2.6. Determination of sodium levels in the skin

The skin samples were carefully placed in a porcelain crucible and positioned in an electric furnace. The crucible was heated gradually until the samples stopped producing smoke. Subsequently, the powdered samples were transferred to a muffle furnace where they underwent a controlled heating process at 190 °C for 24 h. Next, the residue was carefully dried at a temperature of 600 °C for 48 h. Once dried, the residue is dissolved in a 10 % HNO_3 solution. The sodium concentration in the skin is then determined using flame atomic absorption spectrometry (Thermo Fisher, USA).

2.7. Immunofluorescence

Kidney tissues were fixed in 4 % paraformaldehyde overnight at 4 °C. The fixed specimens were rinsed three times with PBS and dehydrated overnight at 4 °C. After sectioning, the sections were air-dried for 1 h, rinsed three times with PBS, and blocked with 10 % goat serum (Thermo Fisher Scientific) for 1 h. Primary antibodies (1:200 dilution) were added and incubated overnight at 4 °C. After rinsing, secondary antibodies (1:500 dilution) were added and incubated for 1 h at 37 °C. The sections were then rinsed and observed under a fluorescence microscope. Lymphatic vessel density was determined using Weidner's classical counting method, averaging counts from 15 fields of view under a 200× magnification.

2.8. Detection of macrophages in the renal cortex by flow cytometry

Rat kidneys were cut into small pieces (2–4 mm in diameter) and immersed in an enzyme mixture provided by a tissue dissociation kit. After shaking for 2 h at 37 °C (180 rpm), the mixture was filtered through a 70 μm filter membrane. The resulting filtrate was collected and centrifuged for 7 min to adjust the cell concentration to 1×10^6 cells/mL. From the adjusted cell suspension, 100 μL was taken for flow cytometry staining. Different tubes were prepared: a negative control tube without antibody, a CD68 single-label tube with CD68 antibody, a CD11b single-label tube with CD11b antibody, and a CD68 and CD11b double-label tube with both antibodies. After incubation, the tubes were washed with precooled PBS, resuspended in 300 μL of buffer, and analysed by flow cytometry.

2.9. Western blot analysis

Kidney tissues were lysed with a lysis buffer (Beyotime, China) to extract total protein. The protein concentration was quantified using a BCA kit (Biosharp, China). Subsequently, the proteins were separated by 10 % SDS–PAGE and transferred onto polyvinylidene fluoride membranes at a constant current of 200 mA for 1.5 h. After blocking with 5 % Quick sealing solution for 1 h, the cells were incubated with primary antibody overnight at 4 °C. Then, the membranes were probed with appropriate secondary antibodies for 2 h. The protein bands were visualized using an enhanced chemiluminescence kit and imaged using a ChemiDoc Imaging System (General Electric Company, CT, USA). Optical density analysis was performed on each strip using ImageJ software (Bio-Rad, CA, USA).

2.10. Real-time quantitative PCR analysis

Total RNA from kidney tissues was extracted using TRIzol reagent (Thermo Fisher). Subsequently, the RNA was reverse transcribed into cDNA using the PrimeScript One-Step RT-PCR Kit. RT–PCR was performed on an Applied Biosystems Step One Plus RT–PCR System. The sequences of the oligonucleotides utilized for quantitative PCR are listed in Table 1.

2.11. Statistical analyses

All the data were processed with GraphPad Prism 8.0 software and are presented as the mean ± standard deviation. Comparisons between groups were analysedd using one-way ANOVA, and statistical significance was set at $P < 0.05$.

3. Results

3.1. DSS has therapeutic effects on ADR-induced NS model rats

The results showed that the ALB and TP levels in the model group were significantly lower than those in the normal group ($P < 0.01$). In contrast, compared with those in the model group, the TP and ALB levels in the DSS, lenvatinib, and amiloride groups increased. (Fig. 1A and B). Compared with those in the control group, TC, TG, BUN, and CR were significantly greater in the model

Table 1
Primer sequences.

Gene	Forward primer	Reverse primer
VEGF-C	CTGGCGTGTTCCTTGCTC	GCTCCTCCAGGTCTTTGC
VEGFR-3	CCTGCCATACGCCACATCAT	TGCATGAAGCCATCCTCCTC
GAPDH	TATCGGACGCCTGGTTAC	CTGTGCCGTTGAACTTGC

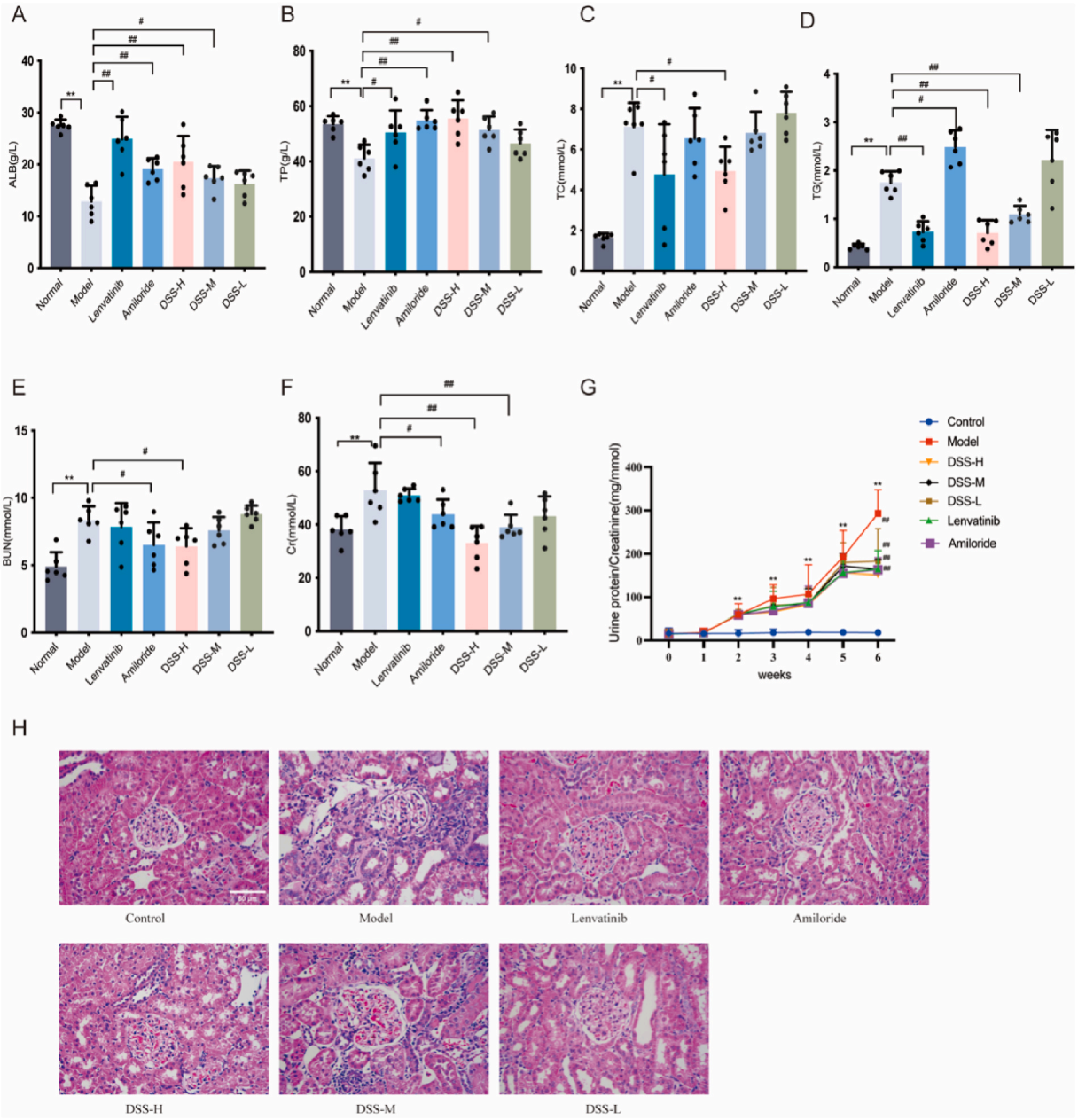

Fig. 1. Effect of DSS on Biochemical Parameters in Rats with NS.**(A-F)**Serum levels of ALB, TP, TC, TG, BUN, CR. **(G)** Excretion curve of urinary proteins. **(H)** Histopathological analysis of the HE-stained kidney sections of rats in each group (magnification × 400). Data are shown as mean ± SD (n = 6). $^{*}P < 0.05$ vs. control, $^{**}P < 0.01$ vs. control, $^{\#}P < 0.05$ vs. model, $^{\#\#}P < 0.01$ vs. model.

group (P < 0.01, Fig. 1C–F), However, DSS and amiloride treatment abrogated these increases. Proteinuria is also a critical biomarker for NS. As expected, NS model rats presented severe proteinuria as evidenced by the remarkable increase in the excretion of urinary protein compared with normal rats (P < 0.01). The administration of DSS, lenvatinib, and amiloride markedly reduced the level of urinary protein in NS model rats (P < 0.01, Fig. 1G).

3.2. DSS alleviates renal lesions in rats with NS

Kidney pathological sections from rats in each group were observed under a 400x high-power microscope (Fig. 1H). The HE staining results showed that the model group rats exhibited glomerular atrophy or disappearance, capillary ring folding, extensive protein-like degeneration of renal tubular cells, massive immune complex deposition and inflammatory infiltration. Compared with

those in the model group, the symptoms of renal histopathological damage in the rats in the levatinib, amiloride, and DSS groups showed different degrees of amelioration improvement, with the high-dose DSS group showing the greatest amelioration of kidney damage.

3.3. The effect of DSS on sodium levels in the urine, blood, and skin of rats

Compared with that of the rats in the normal group, the urinary sodium excretion of rats in the model group decreased significantly after the second week ($P < 0.01$). However, compared with that in the model group, the urinary sodium excretion in the lenvatinib, amiloride, and DSS groups significantly increased at the end of the 4th week ($P < 0.01$), while there was no significant difference in the low-dose of DSS group (Fig. 2A). We further examined the level of plasma sodium level, and the results showed that there was no difference in plasma sodium levels between the groups (Fig. 2B).

However, the level of sodium in the skin of the model group were significantly greater than those in the skin of normal group ($P < 0.01$, Fig. 2C–F). the levels of GAG in the skin of the model group were significantly greater than those in the skin of normal group ($P < 0.01$, Fig. 2, F). DSS reduced the levels of skin sodium and GAG in the skin, especially in the skin of rats in the DSS-H group.

3.4. The number of macrophages in the renal cortex

The flow cytometry results showed (Fig. 3A–H) that compared with those in the normal group, the number of macrophages in the model group was significantly greater ($P < 0.01$). In fact, after the administration of DSS, the number of macrophages in the renal cortex was significantly reduced ($P < 0.01$), especially in the DSS-H group. In addition, amiloride and levantinib can also reduce the number of macrophages.

3.5. Expression of TonEBP, VEGF-C, VEGFR-3, and LYVE-1 proteins, VEGF-C mRNA, and VEGFR-3 mRNA in the renal cortex

We further explored the mechanism by which DSS reduces the skin sodium concentration. We first evaluated the expression of TonEBP, VEGF-C, VEGFR-3, and LYVE-1 using western blotting (Fig. 4A–E). The results showed that the expression of TonEBP, VEGF-

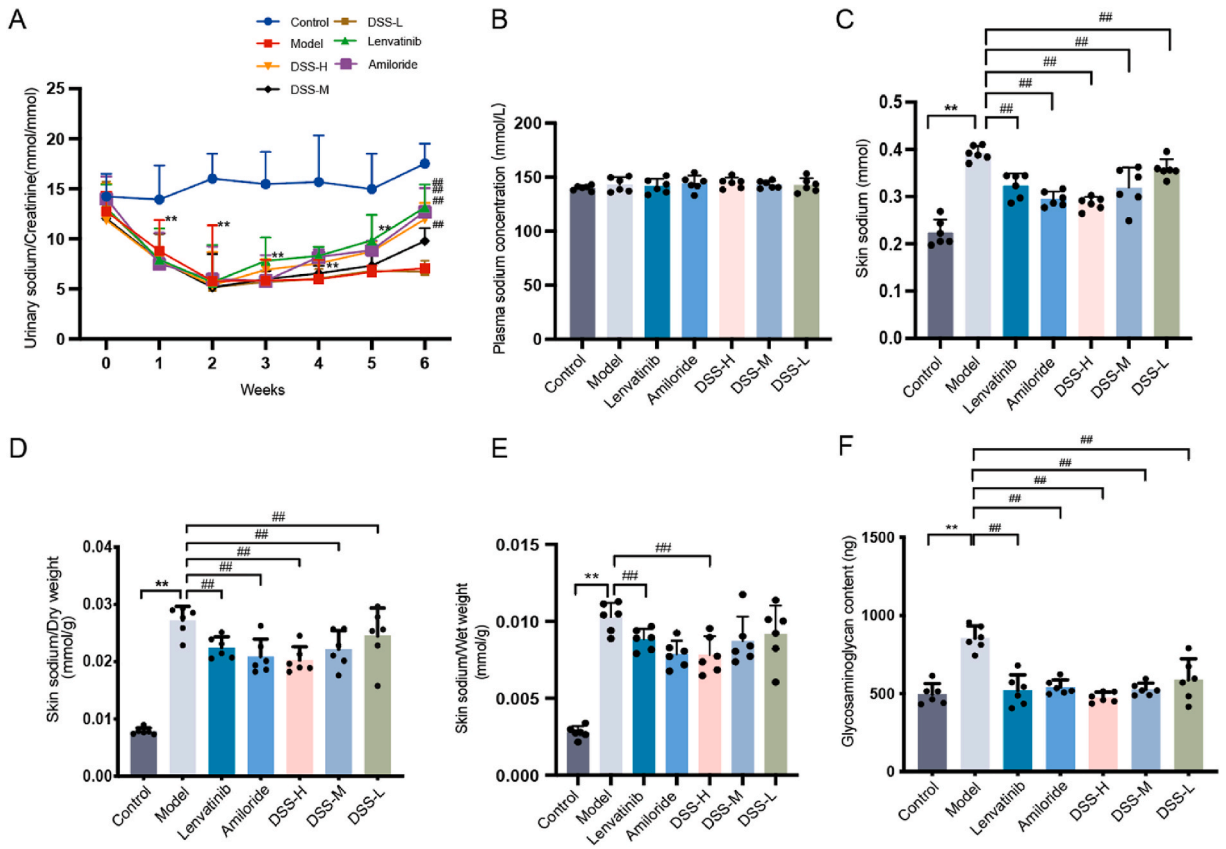

Fig. 2. Effect of DSS on blood and urine sodium levels and skin sodium content in rats with NS. **(A)** Urinary sodium excretion in rats with NS. **(B)** Sodium concentration in plasma. **(C–E)** The content of sodiumin the skin. **(F)** The content of GAG in rat skin. Data are shown as mean ± SD (n = 6). $^{*}P < 0.05$ vs. control, $^{**}P < 0.01$ vs. control, $^{\#}P < 0.05$. vs. model, $^{\#\#}P < 0.01$ vs. model.

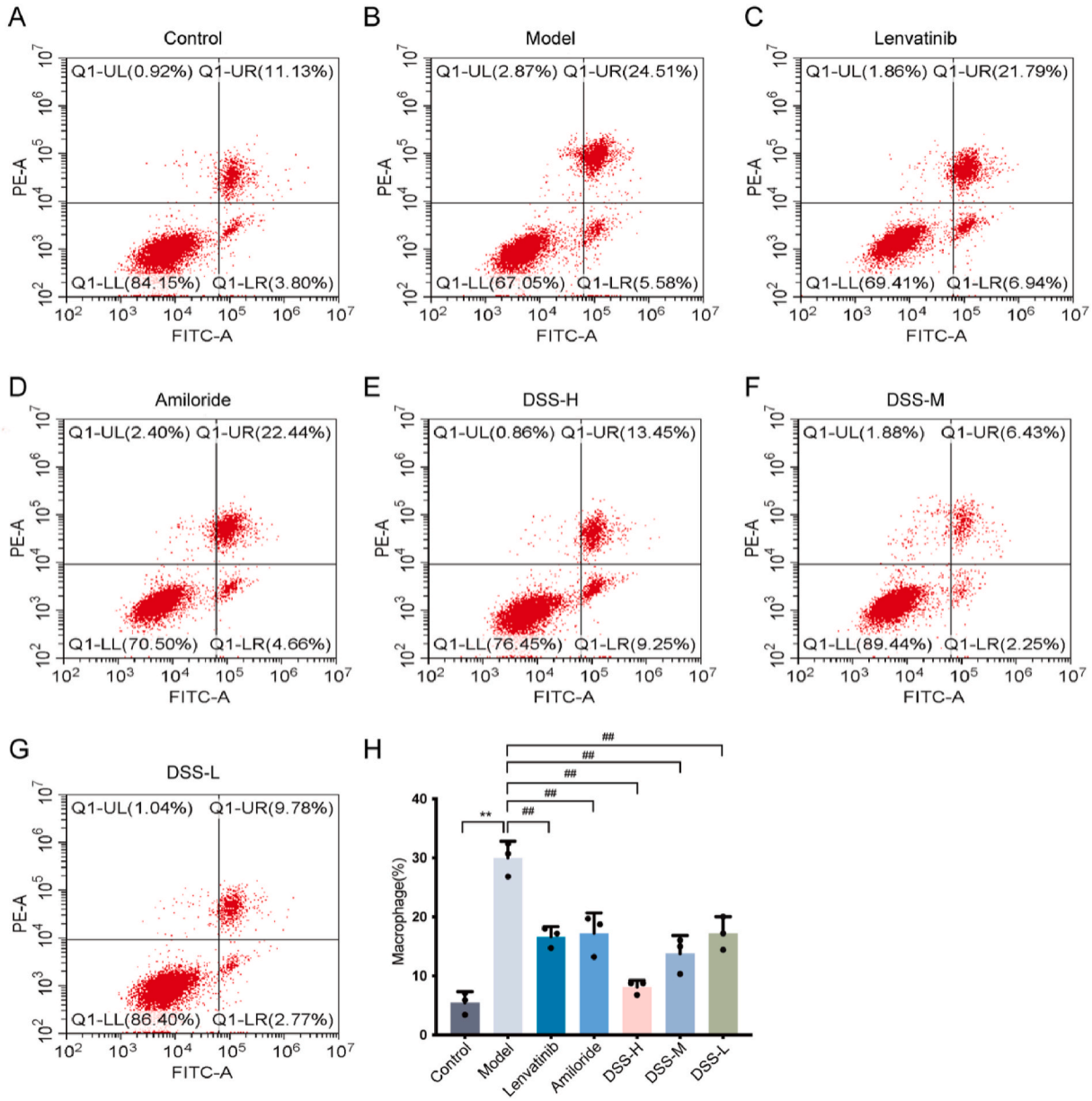

Fig. 3. Effect of DSS on changes in renal cortical macrophage content in rats with NS. **(A–H)** Detection of macrophages in Renal cortex by flow cytometry. Data are shown as mean ± SD (n = 3). $^{*}P < 0.05$ vs. control, $^{**}P < 0.01$ vs. control, $^{\#}P < 0.05$, vs. model, $^{\#\#}P < 0.01$ vs. model.

C, VEGFR-3, and LYVE-1 was increased in the model group ($P < 0.01$). We further examined the expression of VEGF-C mRNA and VEGFR-3 mRNA (Fig. 4F and G), and the results showed that the expression of VEGF-C mRNA and VEGFR-3 mRNA was significantly increased in the model group ($P < 0.05$). DSS can reduce the mRNA expression of VEGF-C mRNA and VEGFR-3 mRNA. Moreover, both lenvatinib and amiloride decreased the mRNA expression of VEGF-C mRNA and VEGFR-3.

3.6. Changes in renal cortical lymphatic vessel density

Immunofluorescence (Fig. 5A–H) revealed that the density of renal cortical lymphatic vessels in the model group was significantly greater than that in the normal group. However, following the administration of DSS, amiloride, or levantinib, the density of lymphatic vessels in the kidney cortex was markedly lower than that in the model group.

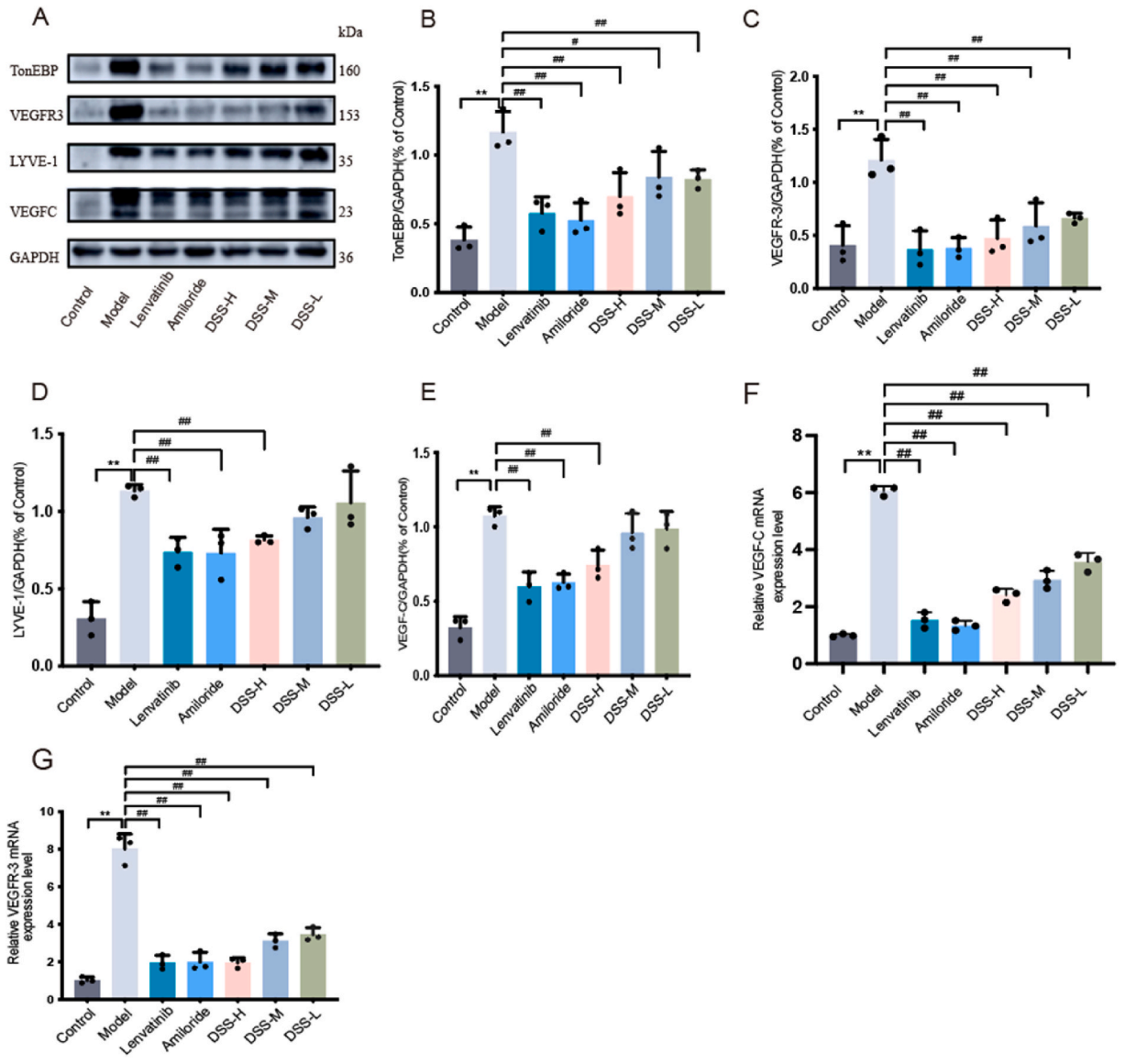

Fig. 4. Effect of DSS on the expression of TonEBP, VEGF-C, VEGFR-3 and LYVE-1 protein and VEGFR-3 and LYVE-1 mRNA in the renal cortex of rats with NS. (**A-E**) Expression of TonEBP, VEGF-C, VEGFR-3 and LYVE-1 protein. (**F** and **G**) Expression of VEGF-C mRNA and VEGFR-3 mRNA in the renal cortex of NS rats. Data are shown as mean ± SD (n = 3). $^{*}P < 0.05$ vs. control, $^{**}P < 0.01$ vs. control, $^{\#}P < 0.05$, vs. model, $^{\#\#}P < 0.01$ vs. model. The original bands of each group of proteins are shown in Supplementary Fig. 1. The original image is in supplementary document.

4. Discussion

Several studies have demonstrated that DSS is effective against NS. However, the mechanisms by which DSS affects NS are still largely unclear. In this study, we explored the possible mechanism by which DSS affects NS. We found that DSS improved renal function in rats with NS. The urinary protein excretion in the model group was considerably greater than that in the control group, and the model group exhibited impaired renal function, which was reflected by increased BUN and SCr levels. However, DSS intervention considerably alleviated proteinuria and hypoalbuminaemia in rats and increased the serum TP concentration in rats. Additionally, the results showed that DSS intervention can reduce kidney damage, as observed under a light microscope. These findings collectively demonstrate that DSS can increase renal function, reduce proteinuria, and ameliorate kidney injury to alleviate ADR-induced NS.

Further observations revealed that DSS increases urinary sodium excretion and reduces the sodium content in the skin. Some studies have shown that sodium can be stored in the body [19,20], especially in the skin, in rats subjected to a high-salt diet. GAG may enable osmotically inactive sodium storage in the skin [21]. However, when sodium retention occurs in rats with NS, can sodium also be stored in the skin? In this study, it was found that sodium could be stored in the skin of NS model rats. Moreover, amiloride can reduce the sodium content in the skin, amiloride is a potassium-retaining diuretic and natriuretic agent that acts by reversibly blocking

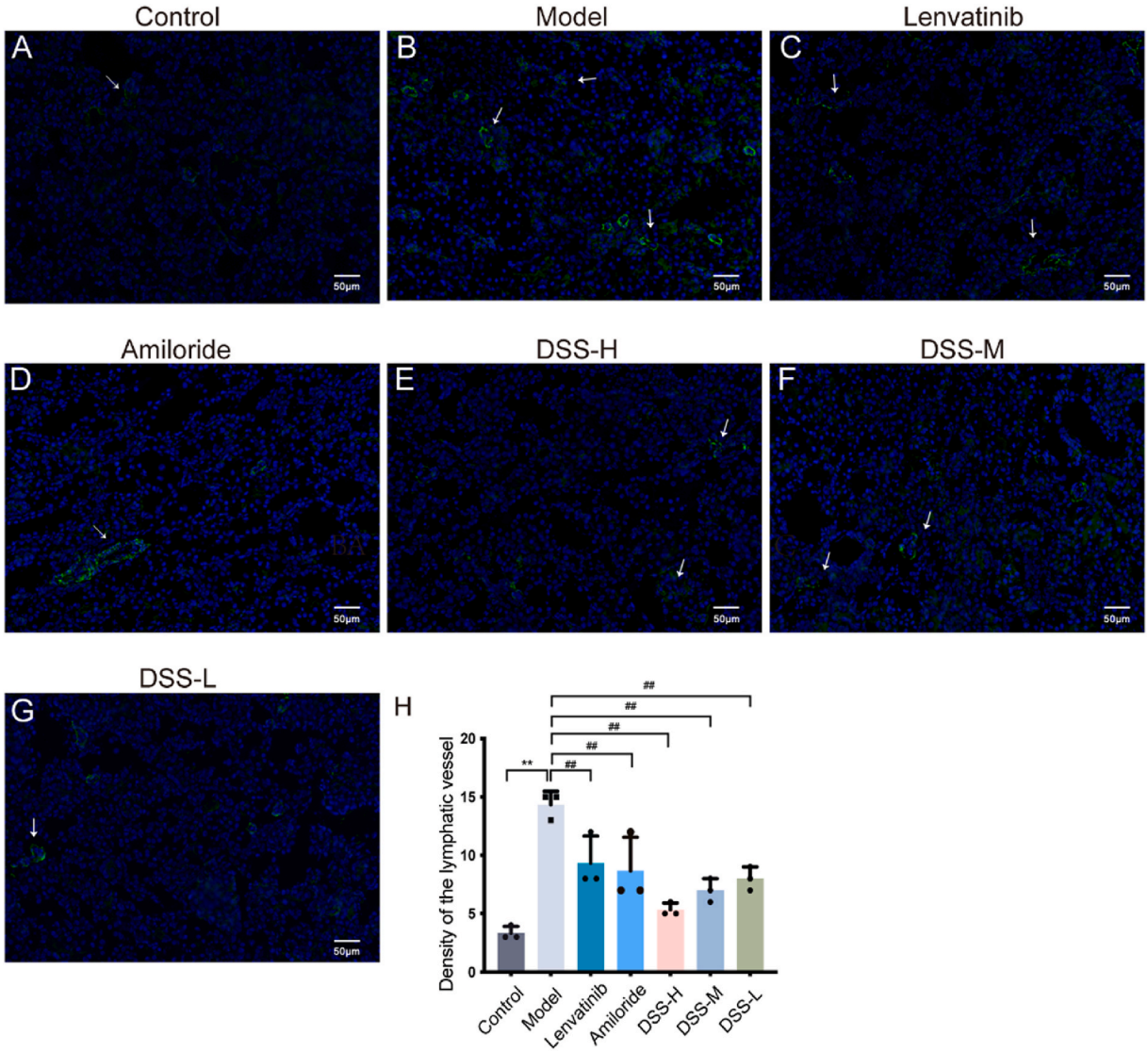

Fig. 5. Effect of DSS on the density of lymphatic vessels in the kidney cortex of NS rats(200 ×). (**A-H**) Density of Lymphatic vessel in Renal cortex of NS rats. Data are shown as mean ± SD (n = 3). $^{*}P < 0.05$ vs. control, $^{**}P < 0.01$ vs. control, $^{\#}P < 0.05$, vs. model, $^{\#\#}P < 0.01$ vs. model.

luminal epithelial sodium channels in the distal tubule and collecting duct [22]. Therefore, amiloride reduces sodium retention in the NS model rats, which may be one of the mechanisms affecting sodium content in the skin. Levantinib caninhibit the growth of lymphatic vessels by targeting VEGFR-3 [23,24]. The transportation of sodium from the kidney to the skin may be closely related to lymphatic vessel growth. These findings demonstrate that DSS has therapeutic effects on rats with NS and can influence the amount of sodium in the skin. DSS significantly reduces sodium levels in the skin of NS model rats and increases urinary sodium excretion. However, there was no difference in the plasma levels of sodium among the groups, which may be the result of the body's balance of sodium in the blood [20].

Some studies have shown that conditions such as a high-salt diet and chronic kidney disease can also cause sodium to be stored in the skin [25,26]. Studies have shown that sodium storage in the skin can lead to a cascade of reactions. Sodium stored in the skin promotes macrophage accumulation, which in turn causes macrophages to express TonEBP and secrete VEGF-C which binds to VEGFR-3 to promote capillary lymphatic vessel proliferation, thereby storing sodium in the skin [27]. In this study, we also found an increase in renal lymphatic vessel density in NS model rats. The lymphatic vessel is closely related to the transport of sodium in the skin, and levantinib can prevent this from occurring. In addition, similar to skin, VEGF-C-mediated lymphangiogenesis has been observed in the heart and kidney of rodents under high-salt diet intervention [28,29]. The renal lymphatics are located in the cortical area and follow the renal artery outwards towards the larger collecting lymphatics to join the peritoneal lymphatics. The interstitial fluid in the renal cortex consists mainly of capillary filtrate and fluid reabsorbed by the renal tubules. Most of renal lymphatic fluid returns to the circulation through the thoracic duct [30–32]. Thus, under pathophysiological conditions, renal lymphatic dysfunction

is closely associated with renal dysfunction [33]. The results of this study showed that the number of macrophages in the cortex of NS model rats decreased after DSS treatment, and the expression of TonEBP, VEGF-C, VEGFR-3, LYVE-1 protein, and VEGF-C mRNA and VEGFR-3 mRNA was significantly reduced. Moreover, there was a decrease in lymphatic vessel density. The skin-related results showed that the sodium and GAG levels in the skin were significantly decreased after DSS administration.

5. Conclusions

In summary, this study indicated that DSS has a therapeutic effect on rats with NS and affects the sodium content in the skin. The possible mechanism may involve inhibiting the aggregation of renal macrophages and downregulating the expression of TonEBP/VEGF-C/VEGFR-3 in the kidney. Therefore, DSS shows promise as a potential drug candidate for the treatment of NS.

CRediT authorship contribution statement

Qingzhen Xiang: Writing – original draft. **Lianghou Ni:** Investigation. **Zaiping Xu:** Methodology. **Xiaowen Ma:** Methodology. **Yunlai Wang:** Writing – review & editing. **Zihua Xuan:** Methodology. **Fan Xu:** Writing – review & editing, Project administration, Funding acquisition, Conceptualization.

Data availability statement

The Data will be made available upon request.

Ethics statement

This study was approved by the Animal Ethics Committee of the Anhui University of Chinese Medicine (licence number: AHUCM-rats-2021068), and conducted in accordance with relevant ethical standards. All participants provided informed consent to participate in the study.

Declaration of competing interest

The authors declare that they have no known competing financial interests or personal relationships that could have appeared to influence the work reported in this paper.

Acknowledgements

This study was supported by the National Natural Science Foundation of China (81974536 and 82274375), Anhui Provincial Science and Technology Major Project (202203a07020006).

Appendix A. Supplementary data

Supplementary data to this article can be found online at https://doi.org/10.1016/j.heliyon.2025.e42577.

References

[1] A.S. Go, T.C. Tan, G.M. Chertow, Primary nephrotic syndrome and risks of ESKD, cardiovascular events, and death: the kaiser permanente nephrotic syndrome study, J. Am. Soc. Nephrol. 32 (2021) 2303–2314, https://doi.org/10.1681/ASN.2020111583.
[2] A. Bierzynska, H.J. Mccarthy, K. Soderquest, Genomic and clinical profiling of a national nephrotic syndrome cohort advocates a precision medicine approach to disease management, Kidney Int. 91 (2017) 937–947, https://doi.org/10.1016/j.kint.2016.10.013.
[3] D. Roccatello, S. Sciascia, D. Di Simone, New insights into immune mechanisms underlying response to Rituximab in patients with membranous nephropathy: a prospective study and a review of the literature, Autoimmun. Rev. 15 (2016) 529–538, https://doi.org/10.1016/j.autrev.2016.02.014.
[4] N.G. Larkins, I.D. Liu, N.S. Willis, Non-corticosteroid immunosuppressive medications for steroid-sensitive nephrotic syndrome in children, Cochrane Database Syst. Rev. 4 (2020) CD002290, https://doi.org/10.1002/14651858.CD002290.pub5.
[5] G. Bhave, E.G. Neilson, Body fluid dynamics: back to the future, J. Am. Soc. Nephrol. 22 (2011) 2166–2181, https://doi.org/10.1681/ASN.2011080865.
[6] M. Fischereder, B. Michalke, E. Schmockel, Sodium storage in human tissues is mediated by glycosaminoglycan expression, Am. J. Physiol. Ren. Physiol. 313 (2017) F319–F325, https://doi.org/10.1152/ajprenal.00703.2016.
[7] D.N. Muller, N. Wilck, S. Haase, Sodium in the microenvironment regulates immune responses and tissue homeostasis, Nat. Rev. Immunol. 19 (2019) 243–254, https://doi.org/10.1038/s41577-018-0113-4.
[8] P. Nijst, F.H. Verbrugge, L. Grieten, The pathophysiological role of interstitial sodium in heart failure, J. Am. Coll. Cardiol. 65 (2015) 378–388, https://doi.org/10.1016/j.jacc.2014.11.025.
[9] G. Rossitto, S. Mary, J.Y. Chen, Tissue sodium excess is not hypertonic and reflects extracellular volume expansion, Nat. Commun. 11 (2020) 4222, https://doi.org/10.1038/s41467-020-17820-2.
[10] H. Wiig, F.C. Luft, J.M. Titze, The interstitium conducts extrarenal storage of sodium and represents a third compartment essential for extracellular volume and blood pressure homeostasis, Acta Physiol. 222 (2018), https://doi.org/10.1111/apha.13006.

[11] B.N. Bohnert, M. Menacher, A. Janessa, Aprotinin prevents proteolytic epithelial sodium channel (ENaC) activation and volume retention in nephrotic syndrome, Kidney Int. 93 (2018) 159–172, https://doi.org/10.1016/j.kint.2017.07.023.
[12] P. Svenningsen, C. Bistrup, U.G. Friis, Plasmin in nephrotic urine activates the epithelial sodium channel, J. Am. Soc. Nephrol. 20 (2009) 299–310, https://doi.org/10.1681/ASN.2008040364.
[13] M. Schafflhuber, N. Volpi, A. Dahlmann, Mobilization of osmotically inactive Na+ by growth and by dietary salt restriction in rats, Am. J. Physiol. Ren. Physiol. 292 (2007) F1490–F1500, https://doi.org/10.1152/ajprenal.00300.2006.
[14] S.A. Stacker, S.P. Williams, T. Karnezis, Lymphangiogenesis and lymphatic vessel remodelling in cancer, Nat. Rev. Cancer 14 (2014) 159–172, https://doi.org/10.1038/nrc3677.
[15] V. Angeli, H.Y. Lim, Biomechanical control of lymphatic vessel physiology and functions, Cell. Mol. Immunol. (2023), https://doi.org/10.1038/s41423-023-01042-9.
[16] J. Huang, X. Wang, L. Xie, Extract of Danggui-Shaoyao-San ameliorates cognition deficits by regulating DHA metabolism in APP/PS1 mice, J. Ethnopharmacol. 253 (2020) 112673, https://doi.org/10.1016/j.jep.2020.112673.
[17] T. Matsuoka, J. Narumoto, K. Shibata, Effect of toki-shakuyaku-san on regional cerebral blood flow in patients with mild cognitive impairment and Alzheimer's disease, Evid Based Complement Alternat Med 2012 (2012) 245091, https://doi.org/10.1155/2012/245091.
[18] Y. Wang, S. Fan, M. Yang, Evaluation of the mechanism of Danggui-Shaoyao-San in regulating the metabolome of nephrotic syndrome based on urinary metabonomics and bioinformatics approaches, J. Ethnopharmacol. 261 (2020) 113020, https://doi.org/10.1016/j.jep.2020.113020.
[19] J. Titze, A. Dahlmann, K. Lerchl, Spooky sodium balance, Kidney Int. 85 (2014) 759–767, https://doi.org/10.1038/ki.2013.367.
[20] S. Lankhorst, D. Severs, L. Marko, Salt sensitivity of angiogenesis inhibition-induced blood pressure rise: role of interstitial sodium accumulation? Hypertension 69 (2017) 919–926, https://doi.org/10.1161/HYPERTENSIONAHA.116.08565.
[21] J. Titze, M. Shakibaei, M. Schafflhuber, Glycosaminoglycan polymerization may enable osmotically inactive Na+ storage in the skin, Am. J. Physiol. Heart Circ. Physiol. 287 (2004) H203–H208, https://doi.org/10.1152/ajpheart.01237.2003.
[22] W. Shen, M. Alshehri, S. Desale, The effect of amiloride on proteinuria in patients with proteinuric kidney disease, Am. J. Nephrol. 52 (2021) 368–377, https://doi.org/10.1159/000515809.
[23] R. Roskoski Jr., Vascular endothelial growth factor (VEGF) and VEGF receptor inhibitors in the treatment of renal cell carcinomas, Pharmacol. Res. 120 (2017) 116–132, https://doi.org/10.1016/j.phrs.2017.03.010.
[24] V. Makker, D. Rasco, N.J. Vogelzang, Lenvatinib plus pembrolizumab in patients with advanced endometrial cancer: an interim analysis of a multicentre, open-label, single-arm, phase 2 trial, Lancet Oncol. 20 (2019) 711–718, https://doi.org/10.1016/S1470-2045(19)30020-8.
[25] J. Titze, M. Shakibaei, M. Schafflhuber, Glycosaminoglycan polymerization may enable osmotically inactive Na+ storage in the skin, Am. J. Physiol. Heart Circ. Physiol. 287 (2004) H203–H208, https://doi.org/10.1152/ajpheart.01237.2003.
[26] A. Dahlmann, P. Linz, I. Zucker, Reduction of tissue Na(+) accumulation after renal transplantation, Kidney Int Rep 6 (2021) 2338–2347, https://doi.org/10.1016/j.ekir.2021.06.022.
[27] A. Machnik, W. Neuhofer, J. Jantsch, Macrophages regulate salt-dependent volume and blood pressure by a vascular endothelial growth factor-C-dependent buffering mechanism, Nat. Med. 15 (2009) 545–552, https://doi.org/10.1038/nm.1960.
[28] S. Beaini, Y. Saliba, J. Hajal, VEGF-C attenuates renal damage in salt-sensitive hypertension, J. Cell. Physiol. 234 (2019) 9616–9630, https://doi.org/10.1002/jcp.27648.
[29] G.H. Yang, X. Zhou, W.J. Ji, VEGF-C-mediated cardiac lymphangiogenesis in high salt intake accelerated progression of left ventricular remodeling in spontaneously hypertensive rats, Clin. Exp. Hypertens. 39 (2017) 740–747, https://doi.org/10.1080/10641963.2017.1324478.
[30] D.J. Jafree, D.A. Long, Beyond a passive conduit: implications of lymphatic biology for kidney diseases, J. Am. Soc. Nephrol. 31 (2020) 1178–1190, https://doi.org/10.1681/ASN.2019121320.
[31] P.S. Russell, J. Hong, J.A. Windsor, Renal lymphatics: anatomy, physiology, and clinical implications, Front. Physiol. 10 (2019) 251, https://doi.org/10.3389/fphys.2019.00251.
[32] H. Seeger, M. Bonani, S. Segerer, The role of lymphatics in renal inflammation, Nephrol. Dial. Transplant. 27 (2012) 2634–2641, https://doi.org/10.1093/ndt/gfs140.
[33] Y. Sato, M. Yanagita, Immune cells and inflammation in AKI to CKD progression, Am. J. Physiol. Ren. Physiol. 315 (2018) F1501–F1512, https://doi.org/10.1152/ajprenal.00195.2018.